

Developing integrated rate laws of complex self-assembly reactions using Lie symmetry: Kinetics of A β 42, A β 40 and A β 38 co-aggregation

Alexander J. Dear,^{1,2} Georg Meisl,³ Sara Linse,² and L. Mahadevan^{1,*}

¹*School of Engineering and Applied Sciences, Harvard University, USA*

²*Center for Molecular Protein Science, Lund University, 221 00 Lund, Sweden[†]*

³*Centre for Misfolding Diseases, Department of Chemistry,*

University of Cambridge, Lensfield Road, Cambridge CB2 1EW, United Kingdom

(Dated: September 29, 2023)

The development of solutions to the kinetics of homomolecular self-assembly into amyloid fibrils using fixed-point methods, and their subsequent application to the analysis of *in vitro* kinetic experiments, has led to numerous advances in our understanding of the fundamental chemical mechanisms behind amyloidogenic disorders such as Alzheimer’s and Parkinson’s diseases. However, as our understanding becomes more detailed and new data become available, kinetic models need to increase in complexity. The resulting rate equations are no longer amenable to extant solution methods, hindering ongoing efforts to elucidate the mechanistic determinants of aggregation in living systems. Here, we demonstrate that most linear self-assembly reactions are described by the same unusual class of singularly perturbed rate equations, that cannot be solved by normal singular perturbation techniques such as renormalization group. We instead develop a new method based on Lie symmetry that can reliably solve this class of equations, and use it in conjunction with experimental data to determine the kinetics of co-aggregation of the Alzheimer’s disease-associated A β 42, A β 40 and A β 38 peptides. Our method also rationalizes several successful earlier solutions for homomolecular self-assembly kinetics whose mathematical justification was previously unclear. Alongside its generality and mathematical clarity, its much greater accuracy and simplicity compared to extant methods will enable its rapid and widespread adoption by researchers modelling filamentous self-assembly kinetics.

I. INTRODUCTION

Self-assembly of proteins and peptides into amyloid fibrils has been intensively studied in the past 20 years due to its key role in a multitude of increasingly prevalent and incurable human pathologies, such as type-II diabetes, Alzheimer’s and Parkinson’s diseases [1, 2]. The kinetics of the self-assembly process have been found to be well-described by nonlinear ordinary differential equations that, although relatively simple, do not normally possess exact analytic solutions. Instead, great success has been had in developing accurate approximate analytic solutions for several particularly important mechanisms of self-assembly [3–9]. These expressions have been widely fitted to experimental data in order to identify the constituent reaction steps and their associated rate constants for many different proteins under diverse conditions [10]. This has enabled fundamental discoveries about the chemical mechanism behind the formation of both pathological and functional amyloid [11], ranging from A β plaques in Alzheimer’s disease [6, 9, 12] to functional yeast prions in *S. cerevisiae* [13]. Such solutions are also intensively used in the screening of candidate inhibitory drugs for the treatment of these diseases [14].

Now that some of the simplest systems have been characterized, researchers have become increasingly interested in less idealized and more realistic representa-

tions of the self-assembly process, described by more complex kinetic equations. For instance, interactions between different proteins or different forms of a protein during aggregation *in vivo* is expected to be the norm rather than the exception, given that biological environments tend to be highly complex, containing multiple self-assembly-prone species as well as other molecular factors in close proximity. A notable example of this is the co-aggregation of different length-variants and post-translationally modified variants of the Alzheimer’s disease-associated A β peptide [15, 16]. Several of these variants occur *in vivo* at non-negligible concentrations, and have been shown or proposed to have differing effects on both the aggregation rate and the progression of the disease [15–22]. A complete understanding of Alzheimer’s disease will likely require a full understanding of the ways in which these proteins interact during aggregation into fibrils. Although these coaggregation reactions have already been studied experimentally *in vitro* [23, 24], the most popular technique for investigating simpler systems, fixed-point theory [3–6], is incapable of successfully modelling them, limiting the kinetic analysis that could be performed at the time.

In recent work [25], the authors posited that the theory of approximate Lie groups, when appropriately extended, might provide a unifying theoretical basis to a wide range of singular perturbation techniques, including but not limited to the method of multiple scales, and the perturbative renormalization group of Chen, Oono and Goldenfeld (CGO RG). This hypothesis was inspired by the little-known fact that most techniques for the ex-

* lm@seas.harvard.edu

[†] alexander.dear.5353@biochemistry.lu.se

act solution of differential equations (DEs) rely implicitly on the identification and exploitation of exact continuous (Lie) symmetries [26]. This raises the questions: can protein aggregation kinetics be treated in a unified way by Lie symmetry, and can Lie symmetry be used to solve the kinetics of co-aggregation of A β length-variants?

We provide in Appendix A an ultra-brief review of those parts of the Lie group theory of DEs that are needed to understand our results; see ref. [25] for a more detailed review. For more background on Lie group theory for DEs in general, see refs. [26–28].

We first show that the rate equations for protein self-assembly admit perturbation series only for specific initial conditions, and that as a result most standard singular perturbation techniques including CGO RG *cannot* be applied. We develop an alternative approach, based on asymptotic Lie symmetries, for regularizing such “local perturbation” series. Using it we obtain a highly accurate approximate solution to the kinetics of co-aggregation of the key A β length variants A β 42, A β 40, and A β 38. (To aid the reader we provide a reference table of mathematical notation in Appendix F.) We successfully fit this model to an array of published data, revealing hitherto undiscovered features of the mechanisms of co-aggregation of these peptides. Additionally, previously highly successful approximate solutions to homogeneous protein self-assembly kinetics are derivable using the same methodology, putting them on a mathematically explainable footing. Our method will find immediate application in the analysis of kinetic experiments on other more complex biochemical systems involving protein aggregation in model mixtures, *in vivo* or in body fluids, and in the search for drugs that can inhibit critical reaction steps in this process.

II. METHODS

Sec. IIA introduces terminology and the fundamental reaction steps in protein aggregation, and introduces dimensionless parameters. We develop our new technique for the solution of protein aggregation rate equations by Lie symmetry in the remaining Methods sections; these mathematically detailed sections may be skipped by readers interested solely in the results on the co-aggregation of A β variants.

A. Highly generalized rate equations for protein fibril formation reactions

The kinetics of amyloid fibril self-assembly in a closed *in vitro* system can generally be modelled by developing rate equations for the fibril number concentration $P(t)$, and the monomer concentration $m(t)$. Since amyloid fibrils typically contain a small number of monomers per plane, but a very large number of planes per fibril, their aggregation can unsurprisingly be accurately modelled

as a linear self-assembly reaction. As will become apparent, in coaggregating systems it is better to instead use $P(t)$ to denote the concentration of fibril ends, which in homomolecular aggregation reactions is just twice the fibril number concentration. New protein fibrils form from monomer in solution through a slow primary nucleation reaction step (often mediated by third-party interfaces such as the air-water interface [9]), and subsequently elongate rapidly (Fig. 1a). Elongation does not create or remove fibril ends and thus only affects $m(t)$ (decreasing it with rate proportional to $m(t)P(t)$). Since nucleation is much slower than elongation, the monomer lost during nucleation can be ignored and to a good approximation primary nucleation increases only $P(t)$ (with rate proportional to $m(t)^{n_c}$).

Most amyloid-forming systems also feature reaction steps whose rates are proportional to the fibril mass concentration $M(t) = m_{\text{tot}} - m(t)$, sometimes summarised as multiplication processes or secondary processes. Such processes induce autocatalytic amplification in filamentous self-assembly. They include fibril fragmentation (rate $k_-M(t)$) as well as secondary nucleation of new fibrils on the surface of existing fibrils (Fig. 1a; rate proportional to $m(t)^{n_2}M(t)$). Putting this all together, and defining $\mu(t) = m(t)/m_{\text{tot}}$, where m_{tot} is the total concentration of protein molecules in monomers and polymeric fibrils, we have:

$$\frac{dP}{dt} = \alpha_1(\mu)\mu(t)^{n_c} + \alpha_2(\mu)\mu(t)^{n_2}(1 - \mu) \quad (1a)$$

$$\frac{d\mu}{dt} = -\alpha_e(\mu)\mu(t)P(t), \quad (1b)$$

where α_1 , α_2 and α_e are rates of primary nucleation, secondary processes and elongation, that may be modified by additional effects such as catalytic saturation, co-aggregation or inhibition. Defining $\kappa = \sqrt{\alpha_e(1)\alpha_2(1)}$, these may be nondimensionalized using $\tau = \kappa t$ and $\Pi(t) = \alpha_e(1)P(t)/\kappa$, yielding:

$$\frac{d\Pi}{d\tau} = 2\varepsilon \frac{\alpha_1(\mu)}{\alpha_1(1)}\mu(\tau)^{n_c} + \frac{\alpha_2(\mu)}{\alpha_2(1)}\mu(\tau)^{n_2}(1 - \mu(\tau)) \quad (2a)$$

$$\frac{d\mu}{d\tau} = -\frac{\alpha_e(\mu)}{\alpha_e(1)}\mu(\tau)\Pi(\tau), \quad (2b)$$

where $\varepsilon = \alpha_1(1)/2\alpha_2(1)$, which can be interpreted as the relative importance of primary nucleation over secondary processes. Nondimensionalization is important for revealing the underlying structure of differential equations; upon nondimensionalization, the rate equations for many different kinds of protein aggregation reactions ultimately have the form of Eqs. (2).

B. Kinetics of protein aggregation cannot be solved by traditional techniques

Eq. (2) admits a perturbation series in ε only for initial conditions $\{\mu(0) = 1, \Pi(0) = 0\}$, as only then

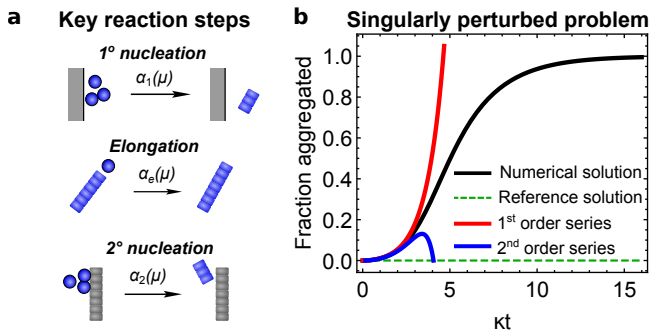


FIG. 1. Demonstration that Eq. (3b) is a singular perturbative solution for the kinetics of linear protein self-assembly. **a:** Key reaction steps involved. **b:** Parameters: $n_2 = 3$, $n_c = 2$, $\varepsilon = 0.01$, $\Pi(0) = 0$, $\mu(0) = 1$, and $\alpha_2 = \alpha_e = 1$. After a short initial time period the first- and second-order perturbation series diverge away from the exact numerical solution to Eqs. (2).

does the term proportional to $1 - \mu$ linearize. This can be generalized to a perturbation series in ε , δ and p , where δ and p enter only the initial conditions as $\{\mu(0) = 1 - \delta, \Pi(0) = p\}$. Pre-multiplying these parameters by perturbation indexing parameter s , to be later set to 1, yields the series:

$$\Pi(\tau) = s \left[\varepsilon(e^\tau - e^{-\tau}) + \frac{\delta}{2}(e^\tau - e^{-\tau}) + \frac{p}{2}(e^\tau + e^{-\tau}) \right], \quad (3a)$$

$$\mu(\tau) = 1 - s \left[\varepsilon(e^\tau + e^{-\tau} - 2) + \frac{\delta}{2}(e^\tau + e^{-\tau}) + \frac{p}{2}(e^\tau - e^{-\tau}) \right]. \quad (3b)$$

Like any singular perturbation series, Eq. (3) is valid only *asymptotically* towards the phase point corresponding to the initial conditions (Fig. 1b). However, a typical singular perturbation series can be solved for arbitrary initial or boundary conditions, permitting this phase point to be moved arbitrarily. Eq. (3) is unusual because its region of validity is instead fixed around $\{\mu(0) = 1, \Pi(0) = 0\}$. We refer to such singular perturbation series, that contain “local” perturbation parameters δ_i originating from the initial or boundary conditions such that the latter may be written $C_j(\delta_i)$, as “local perturbation series”.¹

Eq. (3) can often be regularized into a globally valid solution using the self-consistent method; however, as discussed above, this fails to yield accurate solutions to more complex protein aggregation reactions, such as those involving co-aggregation or inhibition. Aside from the self-

consistent method, CGO RG is the most powerful technique for regularizing singular perturbation problems, and provides a unified theoretical basis for many of the most popular singular perturbation techniques including multiple scale analysis, matched asymptotics and reductive perturbation. However, in ref. [25] we showed that the mathematical basis for CGO RG depends critically on the presence of undetermined constants of integration in the singular perturbation series. Clearly, therefore, CGO RG and related methods cannot be applied to local perturbation series like Eq. (3), since they cannot be solved for arbitrary initial or boundary conditions and thus cannot possess such constants. Instead, a new method must be developed.

C. Exact, approximate and asymptotic Lie symmetries in protein aggregation

Although the intention is to develop a method for application to more complex instances of Eqs (2) (or their higher dimensional equivalents), we illustrate our approach with the simplest possible instance, the kinetics of pure A β 42 aggregation at pH 8.0, in which $\alpha_1 = 2k_n m_{\text{tot}}^{n_c}$, $\alpha_2 = 2k_2 m_{\text{tot}}^{n_2}$ and $\alpha_e = k_+ m_{\text{tot}}$ are μ -independent, yielding:

$$\frac{d\Pi}{d\tau} = 2\varepsilon\mu(\tau)^{n_c} + \mu(\tau)^{n_2}(1 - \mu(\tau)) \quad (4a)$$

$$\frac{d\mu}{d\tau} = -\mu(\tau)\Pi(\tau). \quad (4b)$$

These (and many other instances of Eqs (2)) can be integrated once analytically, and subsequently reduced to quadrature [7]. However, the integration cannot be performed analytically. So, an exact analytic solution for μ is not possible, and Eqs (4) should not possess any non-trivial exact symmetries other than those that yield this quadrature. This can be verified explicitly by their computation using CAS. The objective of a Lie symmetry approach must therefore instead be to derive an approximate analytic solution. However, their explicit computation reveals that Eqs (4) have no non-trivial approximate symmetries (Fig. 2a) either.

Yet, these equations have several approximate analytical solutions, implying they possess some other kind of approximate symmetry property even if they do not possess formal approximate symmetries. Given that these approximate solutions all become more accurate in the limit $\mu \rightarrow 1$, we consider the possibility of Lie symmetries that become exact only *asymptotically* in a given region of phase space (Fig. 2b). The concept of exact “asymptotic symmetries” of DEs, involving dependent and independent variables only, has been investigated in at least two prior mathematical papers [30, 31]. However, a systematic method for their computation was not established, and instead they were computed by guesswork from the DE and its exact symmetries. Hereafter

¹ Note that a local perturbation series is not the same as a perturbation series in the independent variables, which is usually referred to as local analysis [29].

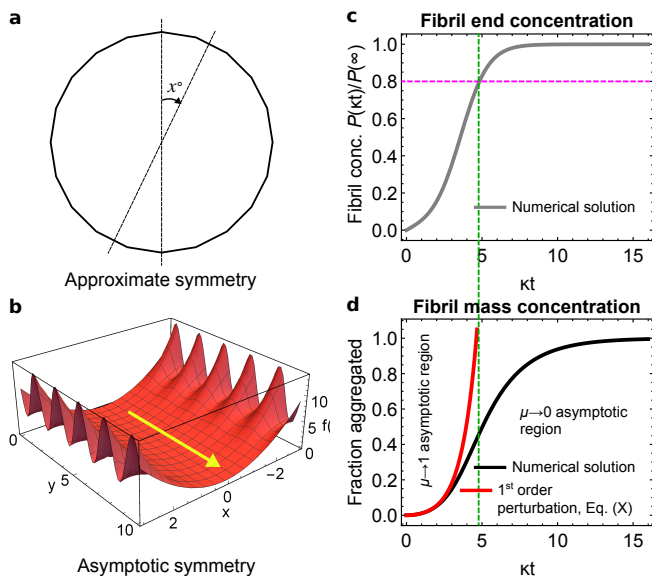


FIG. 2. Illustration of asymptotic symmetries, and asymptotic regions in the kinetics of linear protein self-assembly. **a**: Dodecagons are only approximately invariant under infinitesimal rotational transformations (to $O(\varepsilon)$, where $\varepsilon \sim z \cos \theta$, with θ the external angle and z the side length), which are therefore an approximate Lie symmetry. **b**: $f = x^2 + \varepsilon \sin(\pi y)x^5$ is asymptotically invariant to an arbitrary y -translation in the limit $x \rightarrow 0$; such a translation is thus an asymptotic Lie symmetry. **c**: Numerical solution for fibril end concentration P (rate equation Eq. (1a)); parameters are the same as in Fig. 1. **d**: Numerical solution for normalized fibril mass concentration $1 - \mu$ (rate equation Eq. (1b), black). The $\mu \rightarrow 0$ asymptotic regime, dominated by simple exponential decay of μ , is entered once the fibril number concentration begins to plateau. The local perturbation series (red, Eq. (3b)) is no longer valid in this regime.

we adopt the name “asymptotic” proposed in these papers for this class of symmetries.

Now, we propose asymptotic symmetries of *solutions* to DEs rather than of DEs themselves, and acting on all parameters in the problem, not just the dependent and independent variables. We also propose a systematic method for their computation. If a local approximation to the solution of a DE is available (such as a local perturbation series), then exact or approximate symmetries of this local approximation will be asymptotic symmetries of the solution to the DE. Since these approximations do not contain derivatives, computation of their Lie symmetries can easily be done by hand with no need for the usual computer algebra approaches.

Asymptotic symmetries computed from a local perturbation series are generally only valid near the initial or boundary conditions $C_j(0)$. They are clearly also only valid to the same order in the perturbation parameter as their parent series. (In principle, *exact* asymptotic solution symmetries can instead be calculated if local approximations are available that become exact approaching the phase point around which they were computed.) For ex-

ample, solving Eqs (4) perturbatively to first order with boundary conditions $\{\mu(0) = 1 - \delta, \Pi(0) = \delta + O(\delta^2)\}$, and using again indexing parameter s , yields the following local perturbation series for μ :

$$\mu(\tau) = \mu^{(0)} + s\mu^{(1)} = 1 - s[\varepsilon(e^\tau + e^{-\tau} - 2) + \delta e^\tau]. \quad (5)$$

We can then seek from this a zeroth-order approximate $\mu \rightarrow 1$ asymptotic perturbation symmetry for the exact solution to Eqs. (4), acting solely on parameters ε and δ :

$$\mathbf{X}_{\varepsilon, \delta}^{(0)} = \xi_\varepsilon^{(0)} \frac{\partial}{\partial \varepsilon} + \xi_\delta^{(0)} \frac{\partial}{\partial \delta} \quad (6)$$

Solving $\mathbf{X}_{\varepsilon, \delta}^{(0)}(\mu^{(0)} + s\mu^{(1)}) = 0$ yields the zeroth-order symmetry:

$$\mathbf{X}_{\varepsilon, \delta}^{(0)} = \xi^{(0)} \left(e^\tau \frac{\partial}{\partial \varepsilon} - (e^\tau + e^{-\tau} - 2) \frac{\partial}{\partial \delta} \right), \quad (7)$$

where $\xi^{(0)}$ is an arbitrary function of ε and δ .

Finally, we propose that asymptotic perturbation symmetries may often remain approximately valid throughout the entire phase space of interest. If so, they may in principle be employed to find global approximate solutions. To evaluate whether a given such symmetry is indeed globally valid requires an examination of the bifurcations of the DEs. For protein aggregation the phase space structure is simple, featuring only an attractive fixed point at $\mu = 0$. So, the global dynamics are partitioned into two asymptotic limits: $\mu \rightarrow 1$ and $\mu \rightarrow 0$ (Fig. 2c-d). The boundary between these regions of phase space is marked by the vanishing of the rate of the secondary process, and the resultant plateauing of the fibril number concentration.

$\mu \rightarrow 1$ asymptotic perturbation symmetries are then approximately valid globally under two circumstances. First, if the parameters transformed by the symmetry in response to an increase in the perturbation parameters drop out of the $\mu \rightarrow 0$ kinetics at leading order. For example, Eqs. (4) lose memory of the initial conditions $\{\mu(0) = 1 - \delta, \Pi(0) = \delta + O(\delta^2)\}$ in the $\mu \rightarrow 0$ asymptotic region, becoming independent of δ . Thus, although the $\mu \rightarrow 1$ asymptotic symmetry Eq. (7) transforms δ incorrectly here, it does not matter because the solution no longer depends on δ in this limit, and so Eq. (7) is actually universally valid to zeroth order in ε . The second circumstance is if the boundary between asymptotic regions is sufficiently close to $\mu = 0$, the second region may be neglected. We will see examples of this later.

D. Regularizing local perturbation series using asymptotic symmetries

Globally valid perturbation symmetries can in principle be used to regularize a singular perturbation problem by transforming a known special solution. In Appendix B

we compute such a solution, μ_0 , for Eqs. (4) with boundary conditions $\{\mu(0) = 1 - \delta, \Pi(0) = \delta\}$ when $\varepsilon = 0$ (Eq. (B15)). In the limit that $\delta \ll 1$ this reduces to:

$$\mu_0(\tau, c_1, \delta) = \frac{1}{(1 + \delta e^\tau / c_1)^{c_1}}, \quad (8a)$$

$$c_1 = \frac{3}{2n_2 + 1}. \quad (8b)$$

Since c_1 does not enter into the $\mu \rightarrow 1$ asymptotic dynamics Eq. (5), a global solution to Eqs. (4) for $\delta = 0$ can be obtained simply by integrating the globally valid asymptotic perturbation symmetry Eq. (7) from $(0, \delta)$ to $(\varepsilon, 0)$:

$$\frac{d\varepsilon}{ds} = e^\tau, \quad \frac{d\delta}{ds} = -(e^\tau + e^{-\tau} - 2) \quad (9a)$$

$$\varepsilon = s e^\tau, \quad -\delta = -s(e^\tau + e^{-\tau} - 2) \quad (9b)$$

$$\therefore \delta \rightarrow \varepsilon(e^\tau + e^{-\tau} - 2)/e^\tau. \quad (9c)$$

Replacing δ in Eq. (8) accordingly yields:

$$\mu(\tau) = \frac{1}{\left(1 + \frac{\varepsilon}{c_1}(e^\tau + e^{-\tau} - 2)\right)^{c_1}}, \quad (10)$$

with c_1 defined as before.

The same special solution is often available for the more complicated Eqs. (2) with arbitrary initial conditions when $\varepsilon = 0$ and $p = p_0$ (with p_0 a function of δ defined in Appendix B). This requires that α_1 , α_2 and α_e depend on a parameter d in such a way that $d = 0$ reduces them to finite constants. An asymptotic perturbation symmetry connecting (c_1, δ) with (d, ε, p) may then be used to transform the special solution Eq. (8) to a general solution to Eqs. (2).

Because this kind of symmetry does not transform the dependent and independent variables, a shortcut in this procedure may be taken: it is not necessary to explicitly compute the symmetry and its finite transformations. To see why, suppose such a symmetry connecting (c_1, δ) with (d, ε) has been found. From these, finite transformations taking $(\tilde{c}_1, \tilde{\delta}, 0, 0)$ to $(c_1, \delta, d, \varepsilon)$ can be calculated. Whatever they may be, they can always be expressed in inverse form as $\tilde{\delta} = g_\delta(\tau, c_1, \delta, d, \varepsilon)$, $\tilde{c}_1 = g_{c_1}(\tau, c_1, \delta, d, \varepsilon)$ where a tilde over a parameter signifies it is at its pre-transformation value. Our global solution is then $\mu_0(\tau, \tilde{c}_1, \tilde{\delta})$. Now, since transforming one asymptotic expansion must yield another, g_δ and g_{c_1} must satisfy:

$$\mu_{0,\text{asy}}(\tau, \tilde{c}_1, \tilde{\delta}) \equiv \mu_{\text{asy}}(\tau, c_1, \delta, d, \varepsilon), \quad (11)$$

where $\mu_{0,\text{asy}}$ is the asymptotic expansion of the special solution μ_0 in this region of phase space, and $\mu_{\text{asy}}(\tau, c_1, \delta, d, \varepsilon)$ is the asymptotic limit of the full dynamics in the same region (e.g. Eq. (3), or a higher-order series). So, the finite transformations can be identified by inspection of μ_{asy} ; a globally valid solution is then obtained by substituting these transformations into Eq. (8).

III. RESULTS

A. Modelling A β 42 aggregation in the presence of A β 40 and A β 38

Monitoring by ThT the co-aggregation of A β 42 with A β 40, A β 37 or A β 38 in 20 mM NaP and 0.2 mM EDTA at pH 7.4 in recent studies [23, 24] revealed that two separate sigmoidal transitions occur in the transformation of monomeric to fibrillar protein (Fig. 3a). Using separate stable isotopes in A β 40 and A β 42, and identification using mass spectrometry, the first transition was established to correspond to the formation of fibrillar A β 42, and the second to the formation of fibrils consisting exclusively of the other peptide, implying no cross-elongation reaction steps occur [23]. Seeding experiments were furthermore used to rule out cross-secondary nucleation. Since the second sigmoid occurs earlier than that observed during the aggregation of its associated shorter peptide in isolation, but the first does not, it was deduced that cross-primary nucleation occurs (Fig. 3c), at a rate much faster than that of primary nucleation of the shorter peptide, but much slower than that of A β 42 primary nucleation. It was also found that the shorter peptide inhibits slightly the aggregation of A β 42 (Fig. 3b), but without bespoke kinetic models of inhibition it was not possible to ascertain whether secondary nucleation or elongation was inhibited, and therefore the nature of the co-aggregation interaction responsible [24].

To identify how the inhibition of A β 42 aggregation by A β xx monomers occurs, we first build explicit kinetic models of A β 42 aggregation in which the A β xx monomer inhibits one of the reaction steps. We use the subscripts a and b to signify concentrations of species consisting of A β 42 and A β xx, respectively, and brackets (a) and (b) to denote the corresponding homomolecular rate constants. Cross-primary nucleation can be neglected since it is much slower than A β 42 primary nucleation.

As in refs. [32, 33], we make the simplifying assumption that the binding of A β xx to A β 42 can be modelled as pre-equilibrium, which is reasonable if the binding target has a low concentration, as is expected given the catalytic nature of the steps in protein aggregation [9]. We may then model inhibition of primary nucleation and elongation using perturbed rates [33]:

$$\alpha_{1,a} = 2k_n(a)m_{\text{tot},a}^{n_c(a)}(1 + m_{\text{tot},b}/K_{I,P})^{-1}, \quad (12)$$

$$\alpha_{e,a} = k_+(a)m_{\text{tot},a}(1 + m_{\text{tot},b}/K_{I,E})^{-1}, \quad (13)$$

where $K_{I,P}$ and $K_{I,E}$ are equilibrium constants for dissociation of type- b monomer from the catalytic sites for type- a fibril primary nucleation and elongation, respectively.

Modelling inhibition of secondary nucleation is more complicated, because A β 42 secondary nucleation is at least partly saturated under the reaction conditions (meaning that monomeric protein binds faster to the fibril surface than surface-bound monomer can convert to

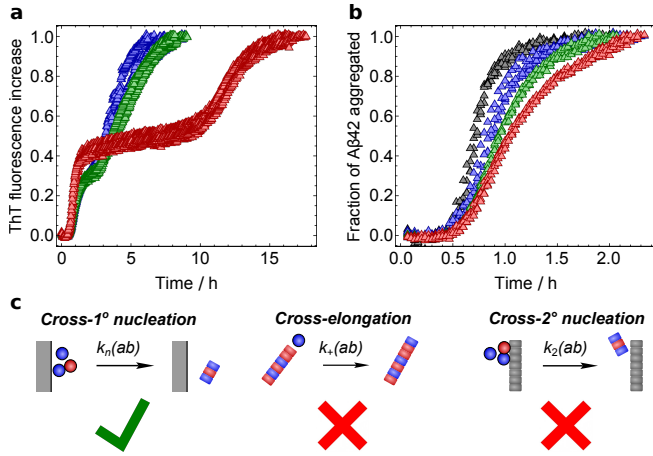


FIG. 3. A β 40 monomer inhibits A β 42 fibril formation. The initial A β 42 monomer concentration is always 3 μ M for the data presented here. The initial A β 40 monomer concentrations are 1 (blue), 3 (green) and 5 (red) μ M. **a**: A β 40 and A β 42 co-aggregation monitored by ThT fluorescence shows separate sigmoids, with the first corresponding to pure A β 42 fibril formation, and the second to pure A β 40 fibril formation. (A β 38 and A β 42 co-aggregation data are qualitatively similar.) **b**: Truncating the data after the first sigmoid and normalizing reveals that monomeric A β 40 has a clear inhibitory effect on A β 42 fibril formation. In addition to the above A β 40 monomer concentrations, included in black is a time series for 3 μ M A β 42 aggregation in isolation (i.e. 0 μ M A β 40). **c**: Earlier studies demonstrate that monomeric A β 42 and A β xx cross-react solely during the primary nucleation reaction step.

new fibrils [6]). Using $\mu_a(t) = m_a(t)/m_{\text{tot},a}$, the rate of secondary nucleation is found (see Appendix C) to be:

$$\alpha_{2,a}(\mu_a) = \frac{2k_2(a)m_{\text{tot},a}^{n_2(a)}\mu_a^{n_2(a)}}{1 + (\mu_a/\mathcal{K}_S(a))^{n_2(a)} + 1/\mathcal{K}_S(ba)}, \quad (14)$$

where $\mathcal{K}_S(a) = K_S(a)/m_{\text{tot},a}$ and $\mathcal{K}_S(ba) = K_S(ba)/m_{\text{tot},b}$ are the dimensionless dissociation constants for types a and b monomers from type- a fibrils.

Thus, the dimensionless rate equations for protein aggregation Eqs. (2) become, using $\Pi_a(t) = 2k'_+(a)P_a(t)/\kappa_a$ and $\tau_a = \kappa_a t$, where $\kappa_a = \sqrt{\alpha_{e,a}\alpha_{2,a}(1)}$:

$$\frac{d\Pi_a}{d\tau_a} = 2\varepsilon_a\mu_a^{n_c(a)+} + \mu_a^{n_2(a)}(1 - \mu_a) \frac{1 + 1/\mathcal{K}_S(a)^{n_2(a)} + 1/\mathcal{K}_S(ba)}{1 + \mu_a^{n_2(a)}/\mathcal{K}_S(a)^{n_2(a)} + 1/\mathcal{K}_S(ba)}, \quad (15a)$$

$$\frac{d\mu_a}{d\tau_a} = -\mu_a(\tau_a)\Pi_a(\tau_a), \quad (15b)$$

where $\varepsilon_a = \alpha_{1,a}/2\alpha_{2,a}(1)$.

B. Solving the kinetics of A β coaggregation

One of the two conditions for applicability of the ‘‘asymptotic symmetry’’ method introduced in this paper for solving differential equations is that there exists a globally valid special solution for a certain choice of parameter values. Since Eqs. (15) are of the same structure as the generic protein aggregation rate equations (Eqs (2)), they must also possess the same special solution, i.e. Eq. (8). This is indeed a valid solution, for the parameter choice $\varepsilon_a = \mathcal{K}_S(a)^{-1} = 0$ (identifying $\tau = \tau_a$ and $n_2 = n_2(a)$).

The other condition for Eqs. (15) to be solvable by this new method has to do with its Lie symmetry basis (namely, that its $\mu \rightarrow 1$ asymptotic symmetry be approximately valid globally); we demonstrate in Appendix D that this condition is indeed satisfied.

As discussed in Sec. IID, although this method depends on Lie group theory, its actual implementation can be performed in a way that requires knowledge only of standard perturbation theory. We will take this approach here. For Eqs. (15), this Lie theory-independent implementation amounts to replacing δ and c_1 in Eq. (8) with functions $\tilde{\delta}$ and \tilde{c}_1 that ensure its Taylor series in δ matches the perturbation series of Eqs. (15) in ε .

Since c_1 does not enter the Taylor series of Eq. (8) to first order, we should perform this matching to second order to ensure optimal accuracy. Calculating the latter by expanding $\mu_a = 1 + \varepsilon\mu_a^{(1)} + \varepsilon^2\mu_a^{(2)}$ and $\Pi_a = \varepsilon\Pi_a^{(1)} + \varepsilon^2\Pi_a^{(2)}$, and substituting these into Eqs. (15), yields:

$$\mu_a(\tau_a) = 1 - \varepsilon_a(e^{\tau_a} + e^{-\tau_a} - 2) + \frac{2 + n'_2(a)}{3}\varepsilon_a^2 e^{2\tau_a} + \mathcal{R}, \quad (16)$$

$$n'_2(a) = n_2(a) \frac{\mathcal{K}_S(a)^{n_2(a)} + \mathcal{K}_S(a)^{n_2(a)}/\mathcal{K}_S(ba)}{1 + \mathcal{K}_S(a)^{n_2(a)} + \mathcal{K}_S(a)^{n_2(a)}/\mathcal{K}_S(ba)}, \quad (17)$$

where \mathcal{R} denotes terms of $O(\varepsilon_a^3)$ or of ε_a^2 that vanish in comparison to the $e^{2\tau_a}$ term in the limit $e^{\tau_a} \gg 1$.

Since this condition determines $\tilde{\delta}$ and \tilde{c}_1 only to $O(\varepsilon^2)$, we are free to require also that the asymptotic expansions in t match, for additional accuracy. Doing so yields $c_1 = 3/(2n'_2(a) + 1)$ and $c_1 [(1 - \delta)^{-1/c_1} - 1] e^{\tau_a} = \varepsilon_a(e^{\tau_a} + e^{-\tau_a} - 2)$. The highly accurate general solution for $M_a(t)$ (see Fig. 4a) is then:

$$\frac{M_a(t)}{m_a(0)} = 1 - \left[1 + \frac{\varepsilon_a}{c_a} (e^{\kappa_a t} + e^{-\kappa_a t} - 2) \right]^{-c_a}, \quad (18a)$$

$$c_a = \frac{3}{2n'_2(a) + 1}. \quad (18b)$$

As $\mathcal{K}_S(a)$ and $\mathcal{K}_S(ba) \rightarrow \infty$ (i.e. when initial monomer concentration is far below the saturation concentration), single-step kinetics are recovered as required.

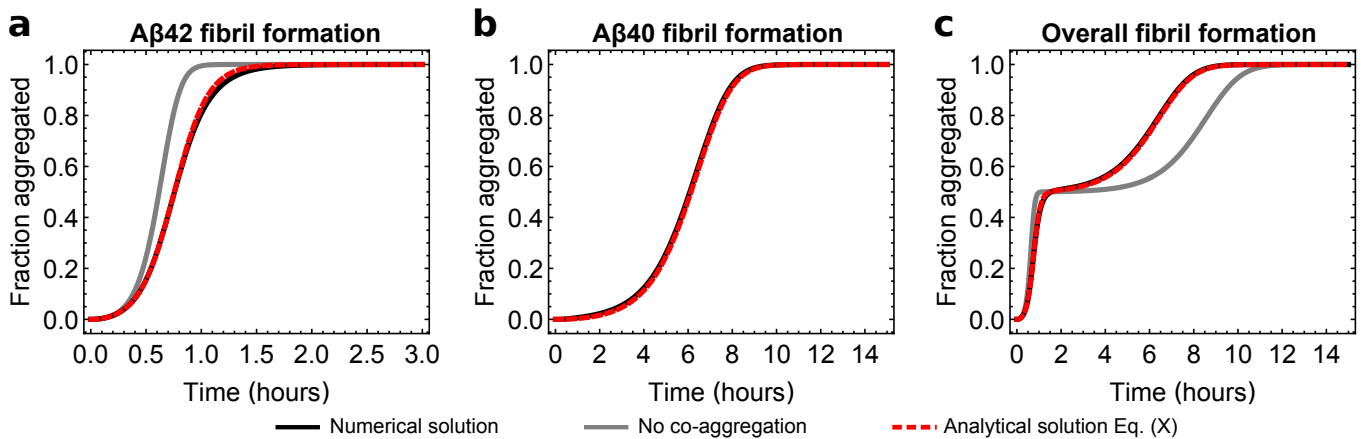


FIG. 4. Analytical solutions to the kinetics of co-aggregation (red, dashed) are highly accurate, tracking the numerical solutions to the rate equations (black) almost exactly. Rate constants are those subsequently determined by fitting experimental data for A β 40-A β 42 coaggregation (see Table II). Numerical solutions in the absence of cross-nucleation (gray) show a clear difference. **a**: The analytical solution to the kinetics of self-assembly of A β 42 fibrils in the presence of A β 40 monomers (Eqs. (18)) closely tracks the numerical solution to Eqs. (15). **b**: Kinetics of self-assembly of A β 40 fibrils (rate equations Eqs. (22a)) are similarly well-described by the analytical solution Eqs. (25). **c**: Kinetics of self-assembly of all fibrils together are consequently modelled well by the combined solution Eq. (26).

C. A β 40 and A β 38 monomers bind to A β 42 fibril surfaces, inhibiting secondary nucleation

We tested Eq. (18) against the data for A β 42-A β 40 co-aggregation and that for A β 42-A β 38 coaggregation, both truncated after the first sigmoid. It is known that at pH 7.4 secondary nucleation of A β 42 is saturated at all but the lowest monomer concentrations, with a dissociation constant of 1.1 μ M [34]. To verify that this value applies here, and that $n_c = n_2 = 2$, we fit in the SI data from homogeneous A β 42 aggregation experiments conducted in the studies from whence the co-aggregation data originates ([23, 24]). Since the other peptide is almost entirely unaggregated during aggregation of A β 42 in the co-aggregation experiments, its concentration is well-approximated as constant.

Allowing inhibition only of primary nucleation by setting $K_{I,E}^{-1} = \mathcal{K}_S(ba)^{-1} = 0$ and fitting $K_{I,P}$ (Fig. 5a), or only of elongation by setting $K_{I,P}^{-1} = \mathcal{K}_S(ba)^{-1} = 0$ and fitting $K_{I,E}$ (Fig. 5b), yielded misfits. However, allowing inhibition only of secondary nucleation by setting $K_{I,P}^{-1} = K_{I,E}^{-1} = 0$ and fitting $\mathcal{K}_S(ba)$ yielded good fits in both systems (Fig. 5c-d), providing strong evidence that A β xx monomers inhibit solely A β 42 secondary nucleation, by binding to the surface of A β 42 fibrils.

The dissociation constant $\mathcal{K}_S(ba)$ was found to be 0.39 μ M for A β 40 monomer on A β 42 fibrils, and 0.86 μ M for A β 38 monomer on A β 42 fibrils. A straightforward comparison of dissociation constants thus suggests that A β 40 monomer has the highest affinity for A β 42 fibril surfaces, followed by A β 38 monomer, with A β 42 monomer perhaps surprisingly in last place. However, the difference between the latter two may not be large enough to be significant relative to experimental error.

Eq. (18) reveals that the kinetics depend on secondary nucleation of A β 42 only via its initial rate:

$$\alpha_{2,a}(1) = \frac{2k_2(a)m_{\text{tot},a}^{n_2(a)}}{1 + (m_{\text{tot},a}/\mathcal{K}_S(a))^{n_2(a)} + m_{\text{tot},b}/\mathcal{K}_S(ba)}. \quad (19)$$

In the absence of saturation, $m_{\text{tot},a} \ll \mathcal{K}_S(a)$ and consequently $\mathcal{K}_S(ba)$ is also the concentration of type- b monomer required to inhibit type- a secondary nucleation by 50% (by binding 50% of catalytic sites). However, saturation breaks this equivalence. Now, inhibition of secondary nucleation depends not on the absolute affinity of type- b monomer to type- a catalytic sites, but its affinity *relative* to that of type- a monomers. When $m_{\text{tot},a} \gg \mathcal{K}_S(a)$, the initial secondary nucleation rate becomes:

$$\alpha_{2,a}(1) \rightarrow \frac{k_2(a)\mathcal{K}_S(a)^{n_2(a)}}{1 + (\mathcal{K}_S(a)/m_{\text{tot},a})^{n_2(a)} m_{\text{tot},b}/\mathcal{K}_S(ba)}. \quad (20)$$

The 50% inhibition concentration is now $m_{\text{tot},b,50\%} = \mathcal{K}_S(ba)(m_{\text{tot},a}/\mathcal{K}_S(a))^{n_2(a)}$. So, the more saturated the kinetics, the higher the concentration of inhibitor is required to achieve the same inhibitory effect.

Since in the solution conditions used here (20 mM NaP, 0.2 mM EDTA, pH 7.4) the A β 42 monomer concentration was 3 μ M, its secondary nucleation is fully saturated and Eq. (20) is a good model of its secondary nucleation in the presence of inhibitors. At the 3 μ M of A β 42 monomer used in Fig. (5), the cross-dissociation constants $\mathcal{K}_S(40,42)$ and $\mathcal{K}_S(38,42)$ correspond to 50% inhibition concentrations of 2.9 and 6.4 μ M, respectively.

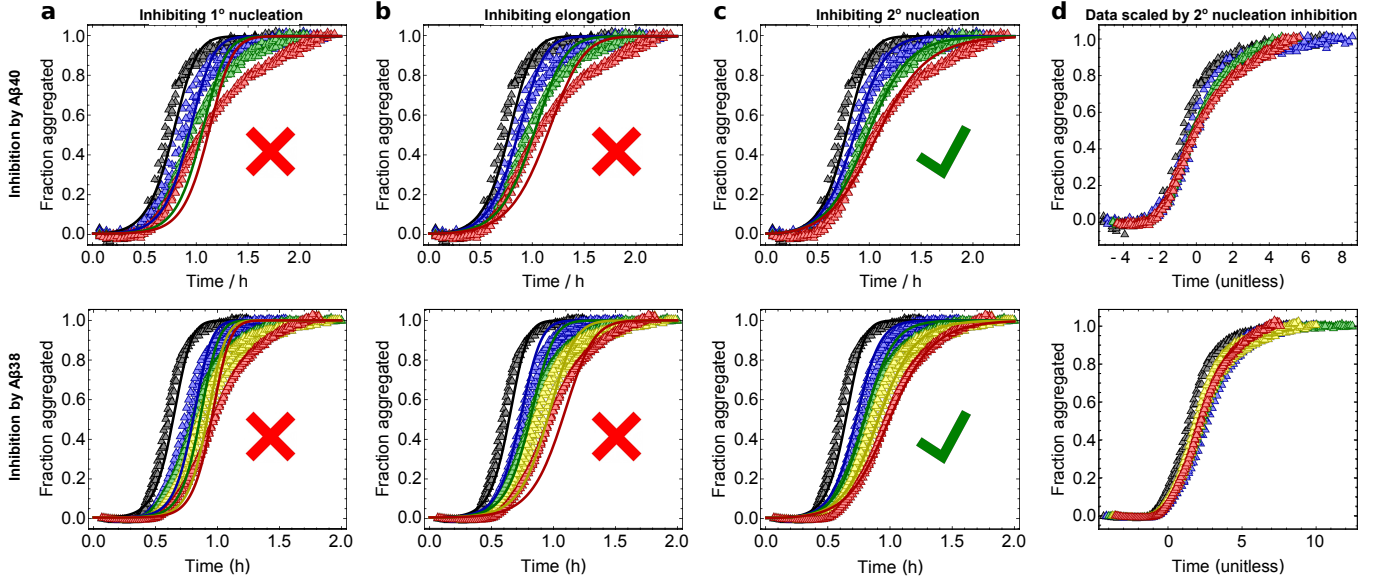


FIG. 5. Determining the origin of the inhibitory effect of A β 40 monomers (top) and A β 38 monomers (bottom) on aggregation of A β 42 (3 μ M). Initial A β 40 monomer concentrations are 0 (black), 1 (blue), 3 (green) and 5 (red) μ M. Initial A β 38 monomer concentrations are 0 (black), 2.5 (blue), 5 (green), 10 (yellow) and 15 (red) μ M. **a**: Misfit of model in which A β xx inhibits primary nucleation (Eqs. (18) with $K_{I,E}^{-1} = \mathcal{K}_S(ba)^{-1} = 0$). **b**: Misfit to models in which A β xx inhibits elongation (Eqs. (18) with $K_{I,P}^{-1} = \mathcal{K}_S(ba)^{-1} = 0$). **c**: Fit of model in which A β xx inhibits secondary nucleation (Eqs. (18) with $K_{I,E}^{-1} = \mathcal{K}_{I,P}^{-1} = 0$). Fitted parameter values are summarized in Tables II-III. **d**: Scaling time by the inhibited secondary nucleation rates collapses the data onto a single curve, confirming that secondary nucleation is the process inhibited.

D. Modelling co-aggregation kinetics of A β 42, A β 40 and A β 38 over the full reaction time course

Having determined the kinetics of A β 42 fibril formation in the presence of A β xx monomer, we now write down the rates governing the kinetics of A β xx fibril formation during an A β xx-A β 42 coaggregation reaction:

$$\alpha_{1,b} = 2k_n(b)m_{\text{tot},b}^{n_c(b)} \quad (21a)$$

$$\alpha_{1,ba} = 2k_n(ba)m_{\text{tot},a}^{n_c(ba)}m_{\text{tot},b}^{n_c(bb)} \quad (21b)$$

$$\alpha_{e,b} = k_+(b)m_{\text{tot},b} \quad (21c)$$

$$\alpha_{2,b} = \frac{2k_2(b)m_{\text{tot},b}^{n_2(b)}}{1 + (m_b(t)/\mathcal{K}_S(b))^{n_2(b)}}, \quad (21d)$$

$\alpha_{1,ba}$ is the rate of production of new type- b fibril ends via cross-primary nucleation, and secondary nucleation can saturate at the monomer concentrations investigated. The A β 40/A β 38 fibril proliferation rate via secondary nucleation is, as usual, $\kappa_b = \sqrt{\alpha_{e,b}\alpha_{2,b}}$.

Using $\tau_b = \kappa_b t$ and $\mu_b = m_b/m_{\text{tot},b}$, the dimensionless rate equations governing aggregation of A β 40/A β 38 are

given by combining Eqs (21) with Eqs (2), yielding:

$$\begin{aligned} \frac{d\Pi_b}{d\tau_b} &= 2\varepsilon_b\mu_b(\tau_b)^{n_c(b)} + 2\varepsilon_{ba}\mu_a(\tau_a)^{n_c(ba)}\mu_b(\tau_b)^{n_c(bb)} \\ &+ \frac{1 + \mathcal{K}_S(b)^{n_2(b)}}{\mu_b(\tau_b)^{n_2(b)} + \mathcal{K}_S(b)^{n_2(b)}}\mu_b(\tau_b)^{n_2(b)}(1 - \mu_b(\tau_b)), \end{aligned} \quad (22a)$$

$$\frac{d\mu_b}{d\tau_b} = -\mu_b(\tau_b)\Pi_b(\tau_b), \quad (22b)$$

where

$$\varepsilon_{ba} = \frac{\alpha_{1,ba}}{2\alpha_{2,b}(1)}, \quad \varepsilon_b = \frac{\alpha_{1,b}}{2\alpha_{2,b}(1)}. \quad (23)$$

Once more, Eq. (8) is a special solution to Eq. (22a) with boundary conditions $\mu_b(0) = 1 - \delta$, $\Pi_b(0) = p_0(\delta)$ when $\{\varepsilon, \mathcal{K}_S(b)^{-1}\} = 0$, defining $\varepsilon = \varepsilon_b + \varepsilon_{ba}$. Because it is also of the same form as Eq. (15), we know that the method of solution by asymptotic symmetries will again apply. Since type- a aggregation is complete before type- b , Eq. (18) may be substituted for $m_a(t)$. Expanding $\mu_b = \mu_b^{(0)} + \varepsilon\mu_b^{(1)} + \varepsilon^2\mu_b^{(2)} + O(\varepsilon^3)$, and $\Pi_b = \varepsilon\Pi_b^{(1)} + \varepsilon^2\Pi_b^{(2)}$, the perturbation series to second order can then be calculated to be (see Appendix E):

$$\begin{aligned} \mu_b(\tau_b) &= 1 - (\varepsilon_b + \varepsilon_{ba}f)(e^{\tau_b} + e^{-\tau_b} - 2) + \mathcal{R} \\ &+ \frac{1}{3} \left(2 + n_2(b) \frac{\mathcal{K}_S(b)^{n_2(b)}}{1 + \mathcal{K}_S(b)^{n_2(b)}} \right) (\varepsilon_b + \varepsilon_{ba}f)^2 e^{2\tau_b}, \end{aligned} \quad (24)$$

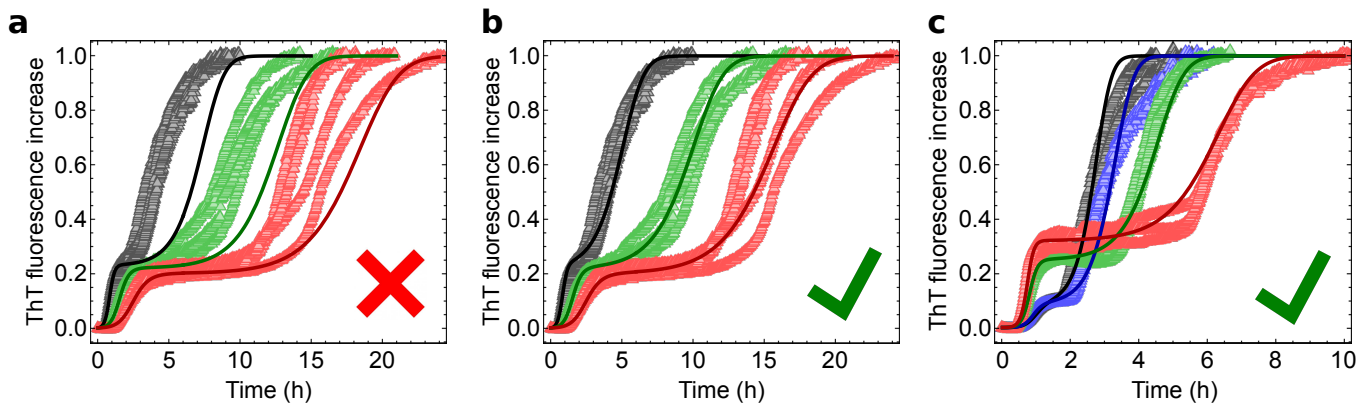


FIG. 6. Fitting the model (Eq. (26)) to the full datasets confirms the importance of cross-nucleation. **a**: Misfit to full dataset for A β 42-A β 40 coaggregation using model in which no cross-primary nucleation occurs. **b**: Fit to full dataset for A β 42-A β 40 coaggregation using model in which cross-primary nucleation occurs; fitted parameter values are summarized in Table II. **c**: Fit to full dataset for A β 42-A β 38 coaggregation using model in which cross-primary nucleation occurs; fitted parameter values are summarized in Table III.

where \mathcal{R} consists of either terms of $\mathcal{O}(\varepsilon^3)$, or terms that vanish in comparison to the dominant terms at each order in the limit $e^\tau \gg 1$. Since before this limit all terms of $\mathcal{O}(\varepsilon)$ and above can be neglected anyway, we may ignore \mathcal{R} for the time being.

Once more, the method can be implemented simply by replacing n_2 and δ in the special solution Eq. (8) with functions $n_2(\varepsilon, \mathcal{K}_S(b)^{-1})$ and $\delta(\varepsilon, \mathcal{K}_S(b)^{-1})$ that ensure its asymptotic expansion in δ matches the above perturbative expansion to second order. Again additionally requiring that the early-time kinetics are recovered, this ultimately yields the following highly accurate approximate solution (Fig. 4b):

$$\frac{M_b(t)}{m_b(0)} = 1 - \left[1 + \frac{\varepsilon_b + \varepsilon_{ba}f}{c_b} (e^{\kappa_b t} + e^{-\kappa_b t} - 2) \right]^{-c_b} \quad (25a)$$

$$c_b = \frac{3}{2n'_2(b) + 1}, \quad n'_2(b) = n_2(b) \frac{\mathcal{K}_S(b)^{n_2(b)}}{1 + \mathcal{K}_S(b)^{n_2(b)}}. \quad (25b)$$

We see immediately that the only effect of cross-nucleation is the addition of $\varepsilon_{ba}f$ to ε_b in the solution, increasing the effective nucleation rate and translating the kinetic curve for type- b monomer to the left. Thus $f < 1$ accounts for the reduction in cross-nucleation rate caused by the depletion of A β 42 monomer.

The kinetics of the overall mixed system as reported upon by ThT fluorescence is finally given by:

$$M_{\text{ThT}}(t) = \phi_a M_a + (1 - \phi_a) M_b, \quad (26)$$

where ϕ_a is related to the fluorescence per unit mass concentration of types a and b fibrils, σ_a and σ_b , by:

$$\phi_a = \frac{\sigma_a}{\sigma_a m_a(0) + \sigma_b m_b(0)}. \quad (27)$$

Testing this analytical solution against a numerical solution of the rate equations reveals it to be highly accurate,

and thus capturing the salient physico-chemical features of this co-aggregating system (Fig. 4c).

Due to inter-repeat variability in fluorescence coefficients, which are highly sensitive to environmental conditions compared to other parameters in the model, we determined σ_a individually for each repeat by inspection of the first normalized plateau height. We then fitted this model to the full double-sigmoidal A β 42-A β 40 dataset, using the parameters previously determined for $k_n(a)k_+(a)$, $k_n(a)k_2(a)$, $n_c(a)$, $n_2(a)$, $n_c(b)$, $n_2(b)$, $K_S(a)$, and $K_S(ba)$. Imposing $k_n(ab) = 0$ (Fig. 6a) yielded a clear misfit, verifying the importance of cross-nucleation. Allowing $k_n(ab) \neq 0$ then yielded good fits to both the full A β 42-A β 40 dataset (Fig. 6b) and the full A β 42-A β 38 dataset (Fig. 6c), and the fitted rates of cross-nucleation confirmed the predictions of refs. [23, 24] that cross-nucleation produces new A β xx fibrils much faster than self-nucleation of A β xx.

IV. DISCUSSION

Our technique may be applied to the majority of plausible rate equations for protein aggregation, provided that the kinetics for the system of interest are sigmoidal in character. It provides extremely accurate results for A β xx co-aggregation. It can likely be applied to any DEs featuring solutions that are sigmoidal in character. It may in future provide a method for the use of analytical basis functions in a systematic way to capture the key features of the solutions to highly nonlinear DEs.

Our formalism also allows various earlier solutions of single-peptide systems to be put on a more rigorous footing. First, the solution presented in ref. [8] is revealed as Eq. (18) with $\mathcal{K}_S(a)^{-1} = \mathcal{K}_S(ba)^{-1} = 0$. Its derivation was claimed to be via CGO RG; however, in reality it was derived implicitly using its $\mu \rightarrow 1$ asymptotic symmetry

properties. Second, the universal solutions in ref. [9] for the kinetics of protein aggregation in which any participating reaction step can undergo enzyme-like saturation were derived by matching second-order perturbative expansions in ε around $\mu = 1$ to that presented in ref. [8]. This is just the method for determining finite transformations of the $\mu \rightarrow 1$ asymptotic symmetries presented above, and is valid for the same reasons.

Although the mathematical justification of the technique is challenging, being rooted in a newly invented sub-field of the specialized field of Lie symmetry analysis of DEs, its practical formulation is clearly very simple. The remarkably simple form of the solutions it produces permits easy analysis of the kinetics. Alongside the lack of alternatives for solving more complicated protein aggregation rate equations, we expect these factors will result in widespread adoption of this new method.

These results are consistent with experimental results showing A β 42 fibrils being coated with A β 40 monomers. For example, A β 42 fibrils with added A β 40 monomer are better dispersed and provide better contrast in cryo-TEM compared to pure A β 42 fibrils [35]. Moreover, the results of SPR experiments show that A β 40 monomers fail to elongate immobilized A β 42 fibrils, yet a saturable binding curve is observed suggesting the binding of A β 40 monomers to the sides of A β 42 fibrils [36].

ACKNOWLEDGMENTS

We acknowledge support from the Lindemann Trust Fellowship, English-Speaking Union (AJD), the Swedish Research Council (SL), the MacArthur Foundation (LM), the Simons Foundation (LM) and the Henri Seydoux Fund (LM). The research leading to these results has received funding from the European Research Council under the European Union's Seventh Framework Programme (FP7/2007-2013) through the ERC grants PhysProt (agreement no. 337969), MAMBA (agreement no. 340890) and NovoNordiskFonden (SL).

Appendix A: Introduction to Lie group theory of differential equations

The theory of Lie groups finds diverse application across theoretical physics. It was originally developed by Sophus Lie as a systematic method for exactly solving nonlinear differential equations (DEs) by exploiting their symmetry properties; however, this application is largely unknown today. Consequently, it is widely believed that nonlinear DEs can be solved only by a combination of guesswork and ad-hoc methods of individually narrow applicability. In fact, most such methods may be derived from the Lie group theory of DEs, which provides a unified and general platform for solving DEs of any kind. Here we give a brief summary of those parts of Lie group

theory of DEs that are utilized in the paper; for a more in-depth treatment, refs. [26, 27] can be consulted.

1. Continuous transformations

A point transformation maps the independent and dependent variables x and y of the object being acted upon to \tilde{x} and \tilde{y} . Point transformations that are indexed by parameter s may be written $\tilde{x} = \tilde{x}(x, y, s)$, $\tilde{y} = \tilde{y}(x, y, s)$. When these are also invertible, contain the identity at $s = 0$, and obey associativity via $\tilde{x}(\tilde{x}(x, y, s), \tilde{y}(x, y, s), t) = \tilde{x}(x, y, s + t)$, they form a one-parameter (or multi-parameter) group of point transformations. Because they are continuous, the infinitesimal transformation exists and can be accessed by expanding around $s = 0$:

$$\tilde{x}(x, y, s) = x + s \left. \frac{\partial \tilde{x}}{\partial s} \right|_{s=0} + \dots = x + s \mathbf{X}x + O(s^2) \quad (\text{A1})$$

$$\tilde{y}(x, y, s) = y + s \left. \frac{\partial \tilde{y}}{\partial s} \right|_{s=0} + \dots = y + s \mathbf{X}y + O(s^2), \quad (\text{A2})$$

where the operator \mathbf{X} is:

$$\mathbf{X} = \xi(x, y) \frac{\partial}{\partial x} + \eta(x, y) \frac{\partial}{\partial y}, \quad (\text{A3})$$

and the elements of the tangent vector $(\xi(x, y), \eta(x, y))$ are:

$$\xi(x, y) = \left. \frac{\partial \tilde{x}}{\partial s} \right|_{s=0}, \quad \eta(x, y) = \left. \frac{\partial \tilde{y}}{\partial s} \right|_{s=0}. \quad (\text{A4})$$

The operator \mathbf{X} is the infinitesimal generator of the point transformation. Integrating the tangent vector over s will yield a finite transformation.

2. What is a Lie symmetry?

A Lie symmetry of an object is a continuous transformation that leaves the object invariant. A rotational symmetry of a square is not a Lie symmetry, as it is discrete and can only be performed in multiples of $\pi/2$ (Fig. 7a). However, a rotational symmetry of a circle can involve any angle, and is thus a Lie symmetry (Fig. 7b). A DE can be viewed as a geometrical object: a manifold consisting of the union of all possible solutions. Often such DEs possess Lie point symmetries: transformations of the dependent and independent variables that leave the overall manifold invariant. Applied to a particular solution (that spans a subspace of the DE manifold) a Lie symmetry of the DE transforms it into another solution (see Fig. 7c). By analogy, a rotational Lie symmetry maps a circle to itself but maps a point on the circle to another point.

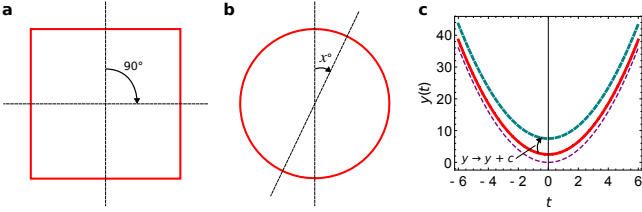


FIG. 7. An overview of Lie symmetries. **a**: Squares have discrete rotational symmetries. These cannot be reduced to infinitesimal form; therefore, they are not Lie symmetries. **b**: Circles can be rotated by any amount; rotation is thus a Lie symmetry of the circle. **c**: In general, symmetries of DEs map solutions to other solutions with different boundary conditions. An arbitrary translation on the y axis is a Lie symmetry of the DE $\dot{y} = 2t$, because this is solved by $y = t^2 + c$, and the translation just changes the value of c , giving the solution to the DE for new boundary conditions.

The ability to express a Lie symmetry in infinitesimal form also makes it possible to calculate systematically the Lie point symmetries possessed by a given object. For DEs this procedure, although algorithmic, can be extremely long-winded because derivatives are not transformed in a straightforward way by Lie point symmetries. To avoid dozens or hundreds of pages of working, it is thus best implemented using computer algebra systems (CAS). On the other hand, for objects without derivatives the procedure is simple. For example, the circle in Fig. 7b may be expressed in polar coordinates as $F = r - c = 0$. In these co-ordinates the generator is $\mathbf{X} = \xi_r \partial / \partial r + \xi_\theta \partial / \partial \theta$. Trivially, solving $\mathbf{X}F = 0$ yields $\xi_r = 0$ and arbitrary ξ_θ : a rotational symmetry. In cartesian co-ordinates $F = x^2 + y^2 - c$, and solving $\mathbf{X}F = 0$ yields η in terms of ξ , giving the generator as follows:

$$0 = \mathbf{X}F = \left(\xi(x, y) \frac{\partial}{\partial x} + \eta(x, y) \frac{\partial}{\partial y} \right) (x^2 + y^2 - c) \quad (\text{A5})$$

$$\therefore \mathbf{X} = \xi(x, y) \left(y \frac{\partial}{\partial x} - x \frac{\partial}{\partial y} \right). \quad (\text{A6})$$

The arbitrary rotational transformation is recovered in cartesian coordinates as expected.

3. Approximate symmetries

A more recent development in the field of Lie group analysis of DEs is the discovery that perturbed DEs can possess “approximate symmetries” [37]. These leave a perturbed DE invariant only to some finite order in the perturbation parameter ϵ . They can be identified by solving:

$$(\mathbf{X}^{(0)} + \epsilon \mathbf{X}^{(1)} + \dots)(F_0 + \epsilon F_1)|_{F_0 + \epsilon F_1 = 0} = 0, \quad (\text{A7})$$

order-by-order [28]. They can often be used to find approximate solutions to perturbed DEs. However, approximate symmetries of DEs are more difficult to compute

than exact symmetries, and there exist few if any CAS implementations of the procedure.

4. Perturbation symmetries

Lie point symmetries of a DE are traditionally thought of as transformations acting on its dependent and independent variables. However, there is nothing to stop us pretending that the perturbation parameter ϵ in a perturbed DE is an independent variable, and searching for symmetries that act on ϵ as well [38]. Doing so can significantly extend the power of the Lie group approach. We have previously termed these “perturbation symmetries” (See ref. [25] for a detailed explanation of these symmetries and this choice of terminology).

Crucially, if a reference solution is known for the perturbation problem with $\epsilon = 0$, this may be converted using a perturbation symmetry of the general solution into a solution valid for arbitrary ϵ . This is because such a symmetry leaves the space of solutions for all possible ϵ unchanged. Thus, acting on a solution for a specific ϵ maps it to another solution with a different ϵ .

Unfortunately, both exact and approximate perturbation symmetries are often extremely difficult or impossible to compute, due to the high dimensionality of the manifold, which defeats most or all CAS implementations. However, we recently developed a method (explained in detail in [25]) that can compute approximate perturbation symmetries of the *solution* to a perturbed DE directly, with far greater ease than earlier methods.

Appendix B: Special solution for $\epsilon = d = 0$

When α_1 , α_2 and α_ϵ are finite constants and $\epsilon = 0$, Eqs. (2) reduce to:

$$\frac{d\Pi}{d\tau} = \mu(\tau)^{n_2} (1 - \mu(\tau)) \quad (\text{B1})$$

$$\frac{d\mu}{d\tau} = -\mu(\tau)\Pi(\tau). \quad (\text{B2})$$

Integrating once, with boundary conditions $\mu(0) = 1 - \delta$, $\Pi(0) = p$ yields for $n_2 > 0$:

$$\Pi(\tau) = \left(p^2 + 2 \frac{(1 - \delta)^{n_2} - \mu(\tau)^{n_2}}{n_2} - 2 \frac{(1 - \delta)^{n_2+1} - \mu(\tau)^{n_2+1}}{n_2 + 1} \right)^{1/2}. \quad (\text{B3})$$

$n_2 = 0$ is also possible and indicates fibril fragmentation rather than secondary nucleation. In this case, we instead obtain:

$$\Pi(\tau) = \left(p^2 - 2 \ln \frac{\mu}{1 - \delta} - 2((1 - \delta) - \mu(\tau)) \right)^{1/2}. \quad (\text{B4})$$

At this point, the problem is reduced to quadrature, with:

$$t = - \int_{1-\delta}^{\mu} \frac{d\mu}{\mu \Pi(\mu)}. \quad (\text{B5})$$

If we choose $p = p_0(\delta) = \delta + O(\delta^2)$, where:

$$p_0 = \sqrt{2 \frac{1 - (1-\delta)^{n_2}}{n_2} - 2 \frac{1 - (1-\delta)^{n_2+1}}{n_2 + 1}}, \quad (\text{B6})$$

then Eq. (B5) reduces to:

$$t = - \int_{1-\delta}^{\mu} \frac{d\mu}{\mu \left(2 \frac{1-\mu^{n_2}}{n_2} - 2 \frac{1-\mu^{n_2+1}}{n_2+1} \right)^{1/2}}, \quad (\text{B7})$$

with the first term in the square root replaced by $-2 \ln \mu$ if $n_2 = 0$. To evaluate this integral, it is necessary to find an accurate approximate expression $g(\mu)$ for the denominator $f(\mu)$. We start by investigating $f(\mu)$ in the interval $[0, 1]$ containing all possible values of μ . We find the following basic properties:

$$f(0) = f(1) = 0 \quad (\text{B8})$$

$$f(\mu) > 0, \quad 0 < \mu < 1 \quad (\text{B9})$$

$$f'(0) = c, \quad f'(1) = -1 \quad (\text{B10})$$

$$f''(\mu) \leq 0, \quad 0 \leq \mu \leq 1. \quad (\text{B11})$$

If we instead restrict our attention to the interval $[0, 1-\delta]$, with small positive δ , we find furthermore that:

$$f(1-\delta) = \delta + O(\delta^2), \quad f'(1-\delta) = -1 + \frac{2n_2 + 4}{3} \delta + O(\delta^2). \quad (\text{B12})$$

Also, there is a single turning point (a maximum) in this interval. When $n_2 = 1$ the maximum value is $f_{\max} = 1/4$, occurring at $\mu_{\max} = 1/2$. As $n_2 \rightarrow \infty$, $f_{\max} \rightarrow c$, and occurs at $\mu_{\max} \rightarrow 1$. Taken together, these results indicate that f is a low hill, rising from 0 at either end of the interval $[0, 1]$ to a value $\leq 1/4$. Thus neither f nor f' have poles.

Such simple behaviour should be adequately captured by the simple functional form:

$$g(\mu) = c_1 \mu^{p_1} + c_2 \mu^{p_2} + c_3, \quad p_2 > p_1 \geq 1. \quad (\text{B13})$$

This is fortunate, because more complicated polynomials in μ are unlikely to lead to an integrable g^{-1} . Now we constrain the parameters in g by matching to the properties of f . First imposing $g(0) = f(0) = 0$ requires $c_3 = 0$. Imposing $g(1-\delta) = f(1-\delta) = \delta + O(\delta^2)$ then leads to $c_2 = -c_1$ and $p_2 - p_1 = 1/c_1 > 0$, so g has the form:

$$g(\mu) = c_1 \mu^{p_1} \left(1 - \mu^{1/c_1} \right). \quad (\text{B14})$$

To inherit the property that $f'(0) > 0$ requires $p_1 = 1$. This is also fortunate, since otherwise g^{-1} would not be

integrable. With this form of g we can already evaluate (and invert) $t = \int_{1-\delta}^{\mu} g^{-1} d\mu$, yielding:

$$\mu(\tau) = \frac{1}{\left(1 + e^{\tau} \left[(1-\delta)^{-1/c_1} - 1 \right] \right)^{c_1}}. \quad (\text{B15})$$

Our asymptotic symmetry transformation method requires that our special solution have the correct $\mu \rightarrow 1$ asymptotic dynamics. Therefore, to choose c_1 , we match $g'(1-\delta) = f'(1-\delta)$ ($g'(1)$ already equals $f'(1) = -1$), yielding finally $c_1 = 3/(2n_2 + 1)$.

(If we had instead matched $g'(0) = f'(0)$, we would have obtained $c_1 = \sqrt{2/(n_2(n_2 + 1))}$. This would give a slightly more accurate solution for $n_2 > 1$, because for larger values of n_2 secondary nucleation decreases significantly at a larger value of μ , and the $\mu \rightarrow 0$ region is more important to the overall dynamics. However, there is not a great difference between these choices for c_1 , with the maximum difference of 6% attained as $n_2 \rightarrow \infty$.)

Appendix C: Kinetic model for amyloid fibril formation with saturating and inhibited secondary nucleation

If type- b monomers can compete with type- a monomers for binding to secondary nucleation sites on type- a fibrils, the total mass concentration of A β 42 fibrils is:

$$M_a = M_a^f + M_a^a + M_a^b, \quad (\text{C1})$$

where M_a^f is the free (unbound) fibril mass concentration, and M_a^a and M_a^b are the mass concentrations of type- a fibrils bound by types a and b monomers, respectively. If, as was done here, the simplifying assumption is made that pre-equilibrium is achieved between bound and unbound states, then we may write:

$$\frac{m_a^{n_2(a)} M_a^f}{M_a^a} = K_S(a)^{n_2(a)}, \quad \frac{m_b^{n_2(ba)} M_a^f}{M_a^b} = K_S(ba)^{n_2(ba)}, \quad (\text{C2})$$

where $K_S(a)^{n_2(a)}$ and $K_S(ba)^{n_2(ba)}$ are the equilibrium constants for the unbinding of types a and b monomers respectively from type- a fibrils. Combining these equations allows us to express the total type- a fibril mass concentration as:

$$M_a = M_a^f \left(1 + m_a^{n_2(a)} / K_S(a)^{n_2(a)} + (m_b / K_S(ba))^{n_2(ba)} \right). \quad (\text{C3})$$

Considering that the rate of generation of new type- a fibrils by secondary nucleation is:

$$r_S = 2k_c M_a^a, \quad (\text{C4})$$

where k_c is some conversion rate constant, this ultimately yields:

$$r_S = \frac{2k_2(a) m_a(t)^{n_2(a)} M_a(t)}{1 + (m_a(t) / K_S(a))^{n_2(a)} + (m_b(0) / K_S(ba))^{n_2(ba)}}, \quad (\text{C5})$$

where $k_2 = k_c/K_S(a)^{n_2(a)}$. Note that with our A β xx-A β 42 system it has been shown that secondary nucleation of A β xx fibrils does not occur on A β 42 fibrils, so clusters of type- b monomers almost certainly do not form on type- a fibrils, and we expect $n_2(ba) = 1$. Indeed, the kinetics of A β 42 aggregation inhibition by A β xx monomers is shown in the main text (Fig. 5c) to be well-described by a model where $n_2(ba) = 1$, i.e. only one A β xx monomer can bind to a given secondary nucleation site on an A β 42 fibril. We provide in the SI a more detailed derivation of the above. Noting that $r_S = \alpha_{2,a}M_a(t)$, nondimensionalization yields finally Eq. (14) in the main text.

Appendix D: Near invariance of $\mu_a \rightarrow 0$ dynamics under $\mu_a \rightarrow 1$ asymptotic symmetry for small $\mathcal{K}_S(a)^{-1}$, ε_a

Asymptotic symmetries involving $\mathcal{K}_S(a)^{-1}$ and ε_a computed from the local perturbation series of Eq. (15) around $\mu_a = 1 - \delta$, $\Pi_a = p_0(\delta)$ are valid globally, provided ε_a is small (as is the case in unseeded A β kinetics, and indeed in most protein aggregation reactions hitherto studied[11]).

For large values of $\mathcal{K}_S(a)^{-1}$, this is because secondary nucleation does not now reduce significantly until $\mu_a \ll 1$. As a consequence, the $\mu_a \rightarrow 0$ asymptotic limit is visited too late during saturating aggregation for its perturbation by the introduction of non-zero $\mathcal{K}_S(a)^{-1}$ and ε to be important for the overall kinetics.

For small values of $\mathcal{K}_S(a)^{-1}$ this is because ε_a and

$\mathcal{K}_S(a)^{-1}$ then drop out of the $\mu \rightarrow 0$ kinetics at leading order, and such symmetries therefore have no effect in this regime. This may be seen as follows. Integrating Eqs. (15) once with $\Pi(\mu = 1) = 1$ yields Π as a function of μ . Taking the limit $\mu \rightarrow 0$ then yields $\Pi(\infty)$:

$$\Pi_a(\infty) = \left(\frac{2(A+B)}{Bn_2(a)} \ln \left[1 + \frac{B}{A} \right] + 4 \frac{\varepsilon_a}{n_c} - \frac{2(A+B)}{A(1+n_2(a))} {}_2F_1 \left[1, 1 + \frac{1}{n_2(a)}, 2 + \frac{1}{n_2(a)}, -\frac{B}{A} \right] \right)^{1/2}, \quad (D1)$$

where $A = 1 + 1/\mathcal{K}_S(ba)$, and $B = 1/\mathcal{K}_S(a)^{n_2(a)}$. In the limit of small $\mathcal{K}_S(a)^{-1}$, and noting that the first-order Taylor series around $z = 0$ of ${}_2F_1[a, b, c, z]$ is $1 + abz/c$, the hypergeometric becomes:

$${}_2F_1 \left[1, \frac{n_2(a)+1}{n_2(a)}, \frac{2n_2(a)+1}{n_2(a)}, -\frac{B}{A} \right] \rightarrow 1 - \frac{n_2(a)+1}{2n_2(a)+1} \frac{B}{A} + O(\mathcal{K}_S(a)^{-2n_2(a)}), \quad (D2)$$

and $\Pi_a(\infty)$ reduces to:

$$\Pi_a(\infty) = \sqrt{\frac{2}{n_2(a)} - \frac{2}{n_2(a)+1}} + O(\mathcal{K}_S(a)^{-n_2(a)}, \varepsilon_a). \quad (D3)$$

Thus, to leading order, $\mu_a \rightarrow 1$ asymptotic symmetries in $\mathcal{K}_S(a)^{-n_2(a)}, \varepsilon_a$ have no effect on the $\mu_a \rightarrow 0$ dynamics.

Appendix E: Perturbation series for μ_b

The differential equations to be solved are Eqs. (22a):

$$\frac{d\Pi_b}{d\tau_b} = 2\varepsilon_b\mu_b(\tau_b)^{n_c(b)} + 2\varepsilon_{ba}\mu_a(\tau_a)^{n_c(ba)}\mu_b(\tau_b)^{n_c(bb)} + \frac{1 + \mathcal{K}_S(b)^{n_2(b)}}{\mu_b(\tau_b)^{n_2(b)} + \mathcal{K}_S(b)^{n_2(b)}}\mu_b(\tau_b)^{n_2(b)}[1 - \mu_b(\tau_b)], \quad (E1a)$$

$$\frac{d\mu_b}{d\tau_b} = -\mu_b(\tau_b)\Pi_b(\tau_b). \quad (E1b)$$

In the limit $e^{\kappa_a t} \gg 1$, such that $\mu_a \rightarrow (1 + \varepsilon_a e^{\kappa_a t}/c_a)^{-c_a}$, the first-order term is calculated as:

$$\mu_b^{(1)}(t) = -\frac{\varepsilon_{ba}}{\varepsilon} \left(e^{\kappa_b t} {}_2F_1 \left[-\frac{\kappa_b}{\kappa_a}, c_a n_c(ba), 1 - \frac{\kappa_b}{\kappa_a}, -\frac{\varepsilon_a}{c_a} \right] - {}_2F_1 \left[-\frac{\kappa_b}{\kappa_a}, c_a n_c(ba), 1 - \frac{\kappa_b}{\kappa_a}, -\frac{\varepsilon_a}{c_a} e^{\kappa_a t} \right] + e^{-\kappa_b t} {}_2F_1 \left[\frac{\kappa_b}{\kappa_a}, c_a n_c(ba), 1 + \frac{\kappa_b}{\kappa_a}, -\frac{\varepsilon_a}{c_a} \right] - {}_2F_1 \left[\frac{\kappa_b}{\kappa_a}, c_a n_c(ba), 1 + \frac{\kappa_b}{\kappa_a}, -\frac{\varepsilon_a}{c_a} e^{\kappa_a t} \right] \right) - \frac{\varepsilon_b}{\varepsilon} (e^{\kappa_b t} + e^{-\kappa_b t} - 2), \quad (E2)$$

where ${}_2F_1[a, b, c, z]$ is the Gaussian hypergeometric function. Bearing in mind the following identity:

$${}_2F_1[a, b, c, z] \equiv \frac{1}{(1-z)^a} {}_2F_1 \left[a, c-b, c, \frac{z}{z-1} \right], \quad (E3)$$

and since $\frac{\varepsilon_a}{c_a} e^{\kappa_a t} \gg 1$ by the time the type- b sigmoid is reached, we may write the second and fourth hypergeometric functions as:

$${}_2F_1\left[-\frac{\kappa_b}{\kappa_a}, c_a n_c(ba), 1 - \frac{\kappa_b}{\kappa_a}, -\frac{\varepsilon_a}{c_a} e^{\kappa_a t}\right] \equiv \left(1 + \frac{\varepsilon_a}{c_a} e^{\kappa_a t}\right)^{\frac{\kappa_b}{\kappa_a}} {}_2F_1\left[-\frac{\kappa_b}{\kappa_a}, 1 - \frac{\kappa_b}{\kappa_a} - c_a n_c(ba), 1 - \frac{\kappa_b}{\kappa_a}, \frac{\frac{\varepsilon_a}{c_a} e^{\kappa_a t}}{1 + \frac{\varepsilon_a}{c_a} e^{\kappa_a t}}\right] \quad (\text{E4})$$

$$\simeq e^{\kappa_b t} \left(\frac{\varepsilon_a}{c_a}\right)^{\kappa_b/\kappa_a} {}_2F_1\left[-\frac{\kappa_b}{\kappa_a}, 1 - \frac{\kappa_b}{\kappa_a} - c_a n_c(ba), 1 - \frac{\kappa_b}{\kappa_a}, 1\right] \quad (\text{E5})$$

$${}_2F_1\left[\frac{\kappa_b}{\kappa_a}, c_a n_c(ba), 1 + \frac{\kappa_b}{\kappa_a}, -\frac{\varepsilon_a}{c_a} e^{\kappa_a t}\right] \equiv \left(1 + \frac{\varepsilon_a}{c_a} e^{\kappa_a t}\right)^{-\frac{\kappa_b}{\kappa_a}} {}_2F_1\left[\frac{\kappa_b}{\kappa_a}, 1 + \frac{\kappa_b}{\kappa_a} - c_a n_c(ba), 1 + \frac{\kappa_b}{\kappa_a}, \frac{\frac{\varepsilon_a}{c_a} e^{\kappa_a t}}{1 + \frac{\varepsilon_a}{c_a} e^{\kappa_a t}}\right] \quad (\text{E6})$$

$$\simeq e^{-\kappa_b t} \left(\frac{\varepsilon_a}{c_a}\right)^{-\kappa_b/\kappa_a} {}_2F_1\left[\frac{\kappa_b}{\kappa_a}, 1 + \frac{\kappa_b}{\kappa_a} - c_a n_c(ba), 1 + \frac{\kappa_b}{\kappa_a}, 1\right]. \quad (\text{E7})$$

In typical secondary nucleating systems such as $A\beta$, $\varepsilon_a \ll 1$. Bearing in mind that ${}_2F_1[a, b, c, z] \rightarrow 1$ as $z \rightarrow 0$, we may simplify the first order perturbation solution further to:

$$\begin{aligned} \mu_b^{(1)}(\tau_b) \simeq & -\frac{\varepsilon_b}{\varepsilon} (e^{\tau_b} + e^{-\tau_b} - 2) - \frac{\varepsilon_{ba}}{\varepsilon} \left(e^{\tau_b} \left(1 - \left(\frac{\varepsilon_a}{c_a}\right)^{\kappa_b/\kappa_a} {}_2F_1\left[-\frac{\kappa_b}{\kappa_a}, 1 - \frac{\kappa_b}{\kappa_a} - c_a n_c(ba), 1 - \frac{\kappa_b}{\kappa_a}, 1\right] \right) \right. \\ & \left. + e^{-\tau_b} \left(1 - \left(\frac{\varepsilon_a}{c_a}\right)^{-\kappa_b/\kappa_a} {}_2F_1\left[\frac{\kappa_b}{\kappa_a}, 1 + \frac{\kappa_b}{\kappa_a} - c_a n_c(ba), 1 + \frac{\kappa_b}{\kappa_a}, 1\right] \right) \right). \quad (\text{E8}) \end{aligned}$$

The simplifications to the second and fourth hypergeometric functions mean this no longer satisfies the initial condition $\mu_b^{(1)}(0) = 0$. To a very good approximation we can restore this limiting behaviour by writing:

$$\mu_b^{(1)}(\tau_b) \simeq -\left(\frac{\varepsilon_b}{\varepsilon} + \frac{\varepsilon_{ba}}{\varepsilon} f\right) (e^{\tau_b} + e^{-\tau_b} - 2), \quad (\text{E9a})$$

$$f = 1 - \left(\frac{\varepsilon_a}{c_a}\right)^{\frac{\kappa_b}{\kappa_a}} {}_2F_1\left[-\frac{\kappa_b}{\kappa_a}, 1 - \frac{\kappa_b}{\kappa_a} - c_a n_c(ba), 1 - \frac{\kappa_b}{\kappa_a}, 1\right]. \quad (\text{E9b})$$

From this, the second order perturbation expansion Eq. (24) can now be derived.

Appendix F: Summary of parameters

TABLE I. Mathematical notation used throughout the paper

Parameter	Definition
\mathbf{X}	Symmetry generator
s	Perturbation indexing parameter
$x_a, x(a)$	Parameter x pertaining to faster-aggregating species a
$x_b, x(b)$	Parameter x pertaining to slower-aggregating species b
m_{tot}	Total monomer concentration
$\mu(\tau) = m(\tau)/m_{\text{tot}}$	Nondimensionalized monomer concentration
$\Pi(\tau) = 2k_+P(\tau)/\kappa$	Nondimensionalized fibril concentration
$\tau = \kappa t$	Nondimensionalized time
$\alpha_1(\mu)$	Primary nucleation rate
$\alpha_2(\mu)$	Secondary nucleation rate
$\alpha_e(\mu)$	Elongation rate
$\kappa = \sqrt{\alpha_e(1)\alpha_2(1)}$	Rate of proliferation of fibrils by secondary processes
$\varepsilon = \alpha_1(1)/2\alpha_2(1)$	Rate of secondary vs primary nucleation
$1 - \delta$	Initial dimensionless monomer concentration
p	Initial dimensionless fibril concentration
k_n	1° nucleation rate constant
k_2	2° nucleation rate constant
k_+	Elongation rate constant
n_c	1° nucleation reaction order
n_2	2° nucleation reaction order
$K_S = K_S/m_{\text{tot}}$	Nondimensionalized dissociation constant
K_S	Dissociation constant for monomers from fibril surfaces

TABLE II. Parameter values for A β 42-A β 40 coaggregation

Parameter	Values (units of μM , h)	
	A β 42	A β 40
k_+k_2	7.6	13.4
k_+k_n	0.021	8.5×10^{-6}
n_2	2	2
n_c	2	3
K_S	1.1	0.081
$n_c(ba)$		2.46
$n_c(bb)$		1.56
$k_n(ba)$		2.5×10^{-4}
$K_S(ba)$		0.39

TABLE III. Parameter values for A β 42-A β 38 coaggregation

Parameter	Values (units of μM , h)	
	A β 42	A β 38
k_+k_2	19.1	30
k_+k_n	0.084	10^{-25*}
n_2	2	2
n_c	0.01	3
K_S	1.1	0.099
$n_c(ba)$		1.84
$n_c(bb)$		0.43
$k_n(ba)$		1.2×10^{-4}
$K_S(ba)$		0.86

TABLE IV. *chosen to be arbitrarily small

- [1] F. Chiti and C. M. Dobson, Protein misfolding, functional amyloid, and human disease. *Annu Rev Biochem* **75**, 333–366 (2006).
- [2] F. Chiti and C. M. Dobson, Protein misfolding, amyloid formation, and human disease: A summary of progress over the last decade. *Annu Rev Biochem* **86**, 27–68 (2017).
- [3] T. P. J. Knowles, C. A. Waudby, G. L. Devlin, S. I. A. Cohen, A. Aguzzi, M. Vendruscolo, E. M. Terentjev, M. E. Welland, and C. M. Dobson, An analytical solution to the kinetics of breakable filament assembly. *Science* **326**, 1533–1537 (2009).
- [4] S. I. A. Cohen, M. Vendruscolo, M. E. Welland, C. M. Dobson, E. M. Terentjev, and T. P. J. Knowles, Nucleated polymerization with secondary pathways. i. time evolution of the principal moments. *J Chem Phys* **135**, 065105 (2011).
- [5] S. I. A. Cohen, M. Vendruscolo, C. M. Dobson, and T. P. J. Knowles, Nucleated polymerization with secondary pathways. ii. determination of self-consistent solutions to growth processes described by non-linear master equations. *J Chem Phys* **135**, 065106 (2011).
- [6] G. Meisl, X. Yang, E. Hellstrand, B. Frohm, J. B. Kirkegaard, S. I. A. Cohen, C. M. Dobson, S. Linse, and T. P. J. Knowles, Differences in nucleation behavior underlie the contrasting aggregation kinetics of the A β 40 and A β 42 peptides. *Proc Natl Acad Sci USA* **111**, 9384–9389 (2014).
- [7] T. C. T. Michaels, S. I. A. Cohen, M. Vendruscolo, C. M. Dobson, and T. P. J. Knowles, Hamiltonian dynamics of protein filament formation. *Phys Rev Lett* **116**, 038101 (2016).
- [8] T. C. T. Michaels, A. J. Dear, and T. P. J. Knowles, Universality of filamentous aggregation phenomena. *Phys Rev E* **99**, 062415 (2019).
- [9] A. J. Dear, G. Meisl, T. C. T. Michaels, M. R. Zimmermann, S. Linse, and T. P. J. Knowles, The catalytic nature of protein aggregation. *J Chem Phys* **152**, 045101 (2020).
- [10] G. Meisl, J. B. Kirkegaard, P. Arosio, T. C. T. Michaels, M. Vendruscolo, C. M. Dobson, S. Linse, and T. P. J. Knowles, Molecular mechanisms of protein aggregation from global fitting of kinetic models. *Nat Protoc* **11**, 252–272 (2016).
- [11] G. Meisl, C. K. Xu, J. D. Taylor, T. C. T. Michaels, A. Levin, D. Otzen, D. Klenerman, S. Matthews, S. Linse, M. Andreassen, and T. P. J. Knowles, Uncovering the universality of self-replication in protein aggregation and its link to disease. *Sci Adv* **from review**, eabn6831 (2022).
- [12] S. I. A. Cohen, S. Linse, L. M. Luheshi, E. Hellstrand, D. A. White, L. Rajah, D. E. Otzen, M. Vendruscolo, C. M. Dobson, and T. P. J. Knowles, Proliferation of amyloid- β 42 aggregates occurs through a secondary nucleation mechanism. *Proc Natl Acad Sci USA* **110**, 9758–9763 (2013).
- [13] J. Yang, A. J. Dear, T. C. T. Michaels, C. M. Dobson, T. P. J. Knowles, S. Wu, and S. Perrett, Direct observation of oligomerization by single molecule fluorescence reveals a multistep aggregation mechanism for the yeast prion protein Ure2. *J Am Chem Soc* **140**, 2493–2503 (2018).
- [14] P. Arosio, M. Vendruscolo, C. M. Dobson, and T. P. J. Knowles, Chemical kinetics for drug discovery to combat protein aggregation diseases. *Trends Pharmacol Sci* **35**, 127 – 135 (2014).
- [15] G. Brinkmalm, W. Hong, Z. Wang, W. Liu, T. T. O’Malley, X. Sun, M. P. Frosch, D. J. Selkoe, E. Portelius, H. Zetterberg, K. Blennow, and D. M. Walsh, Identification of neurotoxic cross-linked amyloid- β dimers in the Alzheimer’s brain. *Brain* **142**, 1441–1457 (2019).
- [16] M. P. Kummer and M. T. Heneka, Truncated and modified amyloid-beta species. *Alzheimer’s Res Ther* **6**, 28 (2014).
- [17] S. Schilling, A. Pradhan, A. Heesch, A. Helbig, K. Blennow, C. Koch, L. Bertgen, E. H. Koo, G. Brinkmalm, H. Zetterberg, S. Kins, and S. Eggert, Differential effects of familial Alzheimer’s disease-causing mutations on amyloid precursor protein (APP) trafficking, proteolytic conversion, and synaptogenic activity. *Acta Neuropathol Commun* **11**, 87 (2023).
- [18] A. T. Welzel, J. E. Maggio, G. M. Shankar, D. E. Walker, B. L. Ostaszewski, S. Li, I. Klyubin, M. J. Rowan, P. Seubert, D. M. Walsh, and D. J. Selkoe, Secreted amyloid β -proteins in a cell culture model include N-terminally extended peptides that impair synaptic plasticity. *Biochemistry* **53**, 3908–3921 (2014).
- [19] O. Szczepankiewicz, B. Linse, G. Meisl, E. Thulin, B. Frohm, C. S. Frigerio, M. T. Colvin, A. C. Jacavone, R. G. Griffin, T. Knowles, D. M. Walsh, and S. Linse, N-terminal extensions retard A β 42 fibril formation but allow cross-seeding and coaggregation with A β 42. *J Am Chem Soc* **137**, 14673–14685 (2015).
- [20] J. T. Jarrett, E. P. Berger, and P. T. Lansbury, The carboxy terminus of the β amyloid protein is critical for the seeding of amyloid formation: Implications for the pathogenesis of Alzheimer’s disease. *Biochemistry (Mosc)* **32**, 4693–4697 (1993).
- [21] J. Wiltfang, H. Esselmann, P. Cupers, M. Neumann, H. Kretschmar, M. Beyermann, D. Schleuder, H. Jahn, E. Rütther, J. Kornhuber, W. Annaert, B. De Strooper, and P. Saftig, Elevation of β -amyloid peptide 2-42 in sporadic and familial Alzheimer’s disease and its generation in PS1 knockout cells. *J Biol Chem* **276**, 42645–42657 (2001).
- [22] J. Näslund, A. Schierhorn, U. Hellman, L. Lannfelt, A. D. Roses, L. O. Tjernberg, J. Silberring, S. E. Gandy, B. Winblad, and P. Greengard, Relative abundance of alzheimer A β amyloid peptide variants in alzheimer disease and normal aging. *Proc Natl Acad Sci USA* **91**, 8378–8382 (1994).
- [23] R. Cukalevski, X. Yang, G. Meisl, U. Weinger, K. Bernfur, B. Frohm, T. P. J. Knowles, and S. Linse, The A β 40 and A β 42 peptides self-assemble into separate homomolecular fibrils in binary mixtures but cross-react during primary nucleation. *Chem Sci* **6**, 4215–4233 (2015).
- [24] G. A. Braun, A. J. Dear, K. Sanagavarapu, H. Zetterberg, and S. Linse, Amyloid- β peptide 37, 38 and 40 individually and cooperatively inhibit amyloid- β 42 aggregation. *Chem Sci* **13**, 2423–2439 (2022).
- [25] A. J. Dear and L. Mahadevan, Approximate lie

- symmetries and singular perturbation theory. *arXiv* **2309.05038** (2023).
- [26] P. Olver, *Applications of Lie Groups to Differential Equations*. Graduate Texts in Mathematics, Springer New York (2000), ISBN 9780387950006.
- [27] H. Stephani, *Differential Equations: Their Solution Using Symmetries*. Cambridge University Press (1990).
- [28] N. Ibragimov and V. Kovalev, *Approximate and Renormgroup Symmetries*. Nonlinear Physical Science, Springer Berlin Heidelberg (2009), ISBN 9783642002281.
- [29] C. M. Bender and S. A. Orszag, *Advanced Mathematical Methods for Scientists and Engineers*. Springer, New York (1999).
- [30] G. Gaeta, Asymptotic symmetries and asymptotically symmetric solutions of partial differential equations. *Journal of Physics A: Mathematical and General* **27**, 437–451 (1994).
- [31] D. Levi and M. A. Rodríguez, Asymptotic symmetries and integrability: The KdV case. *EPL* **80**, 60005 (2007).
- [32] T. C. T. Michaels, C. A. Weber, and L. Mahadevan, Optimal control strategies for inhibition of protein aggregation. *Proc Natl Acad Sci USA* **116**, 14593–14598 (2019).
- [33] T. C. T. Michaels, A. Šarić, G. Meisl, G. T. Heller, S. Curk, P. Arosio, S. Linse, C. M. Dobson, M. Vendruscolo, and T. P. J. Knowles, Thermodynamic and kinetic design principles for amyloid-aggregation inhibitors. *Proc Natl Acad Sci USA* **117**, 24251–24257 (2020).
- [34] G. Meisl, X. Yang, B. Frohm, T. P. J. Knowles, and S. Linse, Quantitative analysis of intrinsic and extrinsic factors in the aggregation mechanism of Alzheimer-associated A β -peptide. *Sci Rep* **6**, 18728 (2016).
- [35] M. Törnquist, Ultrastructural evidence for self-replication of alzheimer-associated a β 42 amyloid along the sides of fibrils. *In press at PNAS* (2020).
- [36] K. Brännström, T. Islam, A. L. Gharibyan, I. Iakovleva, L. Nilsson, C. C. Lee, L. Sandblad, A. Pamrén, and A. Olofsson, The properties of amyloid- β fibrils are determined by their path of formation. *J Mol Biol* **430**, 1940–1949 (2018).
- [37] V. A. Baikov, R. K. Gazizov, and N. H. Ibragimov, Approximate symmetries. *Matematicheskii Sbornik* **178**, 435–450 (1988).
- [38] V. F. Kovalev, V. V. Pustovalov, and D. V. Shirkov, Group analysis and renormgroup symmetries. *J Math Phys* **39**, 1170–1188 (1998).